Journal of Industrial Information Integration 24 (2021) 100223

Contents lists available at ScienceDirect

Journal of Industrial Information Integration

journal homepage: www.elsevier.com/locate/jii

Full length article

Distributed nonlinear state estimation using adaptive penalty parameters with load characteristics in the Electricity Reliability Council of Texas☆

Tierui Zou [a,*], Nader Aljohani [a], Pan Wang [b], Arturo S. Bretas [a], Newton G. Bretas [c]

[a] Department of Electrical & Computer Engineering, University of Florida, Gainesville, FL 32611-6200, USA
[b] School of Automation, Wuhan University of Technology, Wuhan, Hubei 430070, China
[c] Department of Electrical & Computer Engineering, University of Sao Paulo, Sao Carlos, SP 13566-590, Brazil

ARTICLE INFO

Keywords:
Industrial information integration engineering
Multi-area state estimation
Alternating direction method of multipliers
Real-time monitoring

ABSTRACT

As the industries transit towards industrial integration and informatization, the many advantages from interdisciplinary collaborations come with added technical challenge, especially in large scale and complex systems. Different from typical objects, the interconnected power system is the largest system ever built in industrialized world. Since the development of Power System State Estimation (PSSE), it has predominantly been a centralized process that relies on consistent measurement data availability. In a centralized architecture, a single point of failure can impact the entire system. While in distributed topology, the damage could be decreased with exchanging information between neighboring sub-systems. In other fields, distributed architectures have been widely used to avoid this issue, however shallow number of works are reported in PSSE literature. This paper presents a distributed nonlinear PSSE innovation based model that uses an adaptive penalty parameter to improve the convergence and accuracy of the PSSE output such as bus voltage and bus phase. The alternating direction method of multipliers is modified and used to optimize the distributed PSSE while an innovation-based nonlinear model is used to represent the sub-areas composed measurement error. The distributed PSSE algorithm is tested on the IEEE-14 and 118-bus systems using load characteristics from the Electricity Reliability Council of Texas (ERCOT). Numerical results show that the penalty parameter successfully adapts to optimal condition and the objective function has better performance compared to state-of-the-art models after convergence. Easy-to-implement model towards industrialization, built on the weighted least squares (WLS) solution, without hard-to-design parameters, highlight potential aspects for real-life implementation.

1. Introduction

As the fast transition from industries towards industrial integration and informatization, it has significantly increased the amount of information being collected from industrial process. Since the concept of industrial information integration engineering was initially proposed by Xu in 2005 [1–3], it draws a lot of awareness from academic circle and industrial practitioners [4,5]. Since then, industrial information integration engineering has been widely applied in different industrial sectors, including manufacturing, agriculture, environmental protection, and defense industries. The quantity of literature on Industrial Information Integration grew at a remarkable pace [2–5]. Chen has published two literature review papers on industrial information integration engineering [4,5]. Industry 4.0 is the ongoing automation of traditional manufacturing and industrial practices, using modern smart technology. Large-scale machine-to-machine communication (M2M) and the internet of things (IoT) are integrated for increased automation, improved communication, self-monitoring and production of smart machines that can analyze and diagnose issues without the need for human intervention. Accordingly, industrial information integration engineering can be widely applied in different types of industrial sectors, such as wireless communication, hypersonic vehicle, manufacturing, agriculture, and so on. Wang [6] presented a simple but scalable crack detection algorithm that is based on SegNet, which can realize the pixel-wise inspection of concrete or asphalt pavement and bridge deck cracks. Nazarenko [7] discussed the analysis of relevant standards for manufacturing systems which was performed for the Digital Manufacturing Platforms (4DMP) cluster in order to identify those standards that might be relevant for Zero Defects Manufacturing (ZDM), as well as for further projects or manufacturing platform designers.

☆ This work was supported by NSF grant ECCS-1809739.
* Corresponding author.
E-mail address: tieruizou@ufl.edu (T. Zou).

https://doi.org/10.1016/j.jii.2021.100223
Received 2 January 2021; Received in revised form 28 April 2021; Accepted 1 May 2021
Available online 28 May 2021

Meantime, as a sensor, communication, control and other technologies continue to advance into digital age, the power system industry begins to transit to Smart Grids (SG) with integration of increased information as well [8,9]. Power system state estimation (PSSE) is a critical process for real-time monitoring for power industries. This process uses real-time wide-area information to gain awareness of the system state, which is then used in many applications for industrial process, such as power system protection, control and operation. As the power system transitions to the Smart Grid (SG) using new sensors, communications and controls, the role of PSSE only becomes more important to real-time monitoring. The SG will integrate phasor measurement units (PMU), advanced meter infrastructure (AMI) and two way communications networks with the existing Supervisory Control and Data Acquisition (SCADA) systems [10,11]. This industrial integration and informatization trend will enable fully multi-area real-time control and protection. These technologies are critical for the SG of the future, however this transition towards to power industrial integration and information also increases the potential for failures in PSSE [12]. There have already been many reported blackouts on power systems [13–16]. All of these changes have direct impacts on the PSSE process, as more information becomes available for power industries.

While more information is generally considered to be positive in state estimation for many power industries, the distributed power integration planning and evaluation are essential for a more comprehensive understanding of power system operational reliability. How to use integrated information is an important issue. By ensemble learning and Bayesian learning, several novel methodologies based on neural networks are presented recently [17,18]. Meantime, it can present a technical challenge to current PSSE, since it is historically implemented in a centralized architecture. Luenberger observer and Kalman filter are two ways which use a series of measurements to estimate unknown state variables [19,20]. While a typical power system contains thousands of buses, each with their own measurement data, and classical PSSE, usually performed in the control center of power industries estimates the states of all of these buses in a centralized process [21]. The addition of new data can rapidly increase the computational cost of PSSE when done in a centralized way. Furthermore, cyber-attacks often impact the PSSE process by manipulating real-time measurements that the PSSE depends on [22,23]. If a cyber-attack on a single measurement goes undetected, it can have a great impact throughout the operation of industrial process, since PSSE outputs impacts several grid applications [24]. In order to address these issues, considering the centralized architecture, some research has been done towards a distributed PSSE process, which would significantly reduce computational burden of PSSE and enhance power system stability [25,26].

With the restructuring of power industry, distributed generation units have been widely deployed and are being connected to existing distribution networks with the aim of improving power quality, service reliability and energy efficiency of the power systems. Distributed architectures have been used in many other areas, including controls, communications, and machine learning with much success [27–31]. Both centralized and distributed architectures have their pros and cons. Distributed solution may have more robustness and efficiency due to the isolated topology and fast convergence while this solution may lose information of data from neighboring areas. For power industries, distributed solution can also bring better load regulation, increased flexibility, maintainability, redundancy, better power and heat management which are their primary considerations. For PSSE, comparatively with centralized architectures, a shallow number of distributed approaches have been presented in the literature [32–34]. In [35], state estimation within a hierarchical framework was presented, where the local estimation results are globally coordinated with a control center. However, this hierarchical solution has reported poor reliability. [36] presents a distributed architecture for WLS estimation based on Richeardson iterative equations. This method can adapt to different scenarios of topology, however, the convergence performance reported might hinder real-life applications. Authors of [37] presented a multi-area PSSE based on sub-regions individually performing local state estimation while considering a central control center coordinating towards optimal solution. This method though does requires a global communication network. In [38], a distributed PSSE approach is presented based on alternating direction method of multiplier (ADMM). The presented model is linear, which has limited accuracy, and uses a fixed step-size for model solution, which does not optimize convergence. A consensus based approach considering the classical WLS model is presented in [39]. This solution is most interesting and reports improved convergence rates, however it also uses a constant step-size.

In recent years the use of phasor measurement units (PMU) have enabled the development of hybrid measurement models for industrial information integration in power system, considering PMU SCADA mixed observations [40]. Considering such models, PMU angle measurement errors are addressed in [41] considering a limited information exchange between neighboring areas. In [42], a distributed hybrid state estimation model with mixed measurements was presented and solved by the alternating direction multiplier method.

Considering the previously mentioned distributed PSSE solutions, some common aspects can be highlighted. First, all measurement models presented are residual based, where the goal is to minimize the weighted norm of the residual, which has been proven to not represent the mask component of the error [43–46], thus potentially converging to a non optimal solution. Second, considering distributed models solution, coordination is consensus or fixed penalty parameters based, which do not adapt to operation conditions, thus increase computational costs for power industries. On the other hand, centralized power system state estimators based on nonlinear measurement models are used worldwide in nearly all power industries. In addition, there are some research work for distributed power system state estimation. However, most of this work is focusing on linear measurement models which is not able to satisfy the fast transition towards integration and information of power industries. In this paper, otherwise, a nonlinear distributed PSSE is presented by adapting system penalty parameter with integrating the load information from the Electricity Reliability Council of Texas (ERCOT). Further, an alternating direction method of multipliers (ADMM) introduced in [27] is used to create an adaptive penalty parameter. The adaptive penalty parameter is used to ensure the shared states within the distributed PSSE architecture are estimated to be sufficiently close together such that neighboring areas can help each other converge to accurate PSSE solutions. On the other hand, adaptive penalty parameter is used based on primal and dual residue of system optimization to guarantee convergence performance. Therefore, the specific contributions of this work towards the state-of-the-art are threefold:

1. Nonlinear innovation based distributed state estimation model for power industries operation;
2. Adaptive penalty parameter developed with an alternative direction method of multipliers towards fast convergence of distributed architecture.
3. Integrating data characteristics from ERCOT to perform presented solution.

The remaining of this paper is divided as follow. Section 2 presents background information in regards to classical state estimation method used in power industries, such as General Electric company (GE) and Schneider Electric Company (SE). Section 3 presents the data integration of actual load characteristics from Electricity Reliability Council of Texas (ERCOT). Section 4 presents the distributed nonlinear state estimation model. The adaptive penalty parameter approach is presented on Section 5. Case study is presented on Section 6. Section 7 presents the conclusions of this work.

2. Background information

2.1. Problem formulation

A power system is composed of a set of interconnected systems where each monitored area contains a subset of buses that are supervised by a control center. Control centers collects local area measurements, communicate with their neighboring control centers and perform sufficient computational tasks such as state estimation. In a centralized PSSE architecture, information of all areas of the grid, such as system topology and measurement collection, is required in order to estimate the system state. Therefore, computational efficiency will be reduced due to high-dimensional of search space and financial cost increase due to necessary large-scale communication infrastructure. In contrast, a distributed PSSE (D-PSSE) would require minimal information for each control center that is mostly constituted by their local and neighboring state information in order to have an estimate of the system state.

A power system with n buses and m measurements can be modeled as a set of non-linear algebraic equations, as follows:

$$z = h(x) + e, \tag{1}$$

where $z \in \mathbb{R}^m$ is the measurement vector, $x \in \mathbb{R}^N$ is the state variables vector, $h(x) : \mathbb{R}^N \to \mathbb{R}^m, (m > N)$, is a non-linear differentiable function that relates the states to the measurements, and e is the measurement residual vector assumed with zero mean, standard deviation σ and having Gaussian probability distribution.

From (1), one can the rewrite the non-linear algebraic expression for a distributed power system with k areas as:

$$z_k = h_k(x_k) + e. \tag{2}$$

The distributed WLS state estimator searches for the best estimates of the system states x_k which minimizes the cost function:

$$J_k(x_k) = \left\| z_k - h_k(x_k) \right\|^2_{R_k^{-1}} = [z_k - h_k(x_k)]^T R_k^{-1} [z_k - h_k(x_k)]. \tag{3}$$

where R_k is the measurement covariance matrix in area k. $J_k(x)$ is geometrically a norm in the measurements vector space $\mathbb{R}^{m_k}$ of area k. One should notice R_k of each area is a positive definite symmetric matrix where each diagonal element is defined by the magnitude of corresponding measurement. Then, the objective cost function for a distributed state estimation architecture is equal to the sum of individual area functional:

$$\begin{aligned} &\min_{x_k \in \chi_k, x_{kl}} \quad \sum_{k=1}^{K} J_k(x_k), \\ &s.t.\ x_k[l] = x_l[k], \forall\, l \in \Gamma_k, \forall\, k. \end{aligned} \tag{4}$$

For every two neighboring areas k and l, the vector $x_k[l]$ contains states in area k that overlap with area l and ordered as they appear in the state vector x. For example, the state variables in $x_k[l]$ and $x_l[k]$ correspond to the shared state between area k and area l. Non-shared state elements in $x_k[l]$ and $x_l[k]$ will be zero since no information of these elements need to be exchanged. x_{kl} is an auxiliary variable used to be reference state between area k and l. The set Γ_k denotes the areas sharing the same state variables.

Eq. (4) forces adjacent areas to be concordant with their shared variables. To enable a truly decentralized solution, an auxiliary variable x_{kl} is introduced for each pair of neighboring areas k and l ($x_k[l] = x_{kl}, x_l[k] = x_{kl}$). Then, Eq. (4) can be alternatively expressed as:

$$\begin{aligned} &\min_{x_k \in \chi_k, x_{kl}} \quad \sum_{k=1}^{K} J_k(x_k), \\ &s.t.\ x_k[l] = x_{kl}, \forall\, l \in \Gamma_k, k = 1, 2, \ldots, K. \end{aligned} \tag{5}$$

Further illustration will be introduced in next subsection.

2.2. Linear D-PSSE based on alternating direction method of multipliers

Previous research [38] has presented a linear Distributed PSSE model using the ADMM. The method has been successfully applied for distributed optimization problems. One can define the problem as an augmented Lagrange function as follows:

$$\begin{aligned} &Ł(x_k, x_{kl}; v_{k,l}) \\ &= \sum_{k=1}^{K} [J_k(x_k) + \sum_{\ell \in \Gamma_k} (v_{k,l}^T (x_k[l] - x_{kl})) + \rho/2 \left\| x_k[l] - x_{kl} \right\|_2^2] \end{aligned} \tag{6}$$

In ADMM, Lagrange multipliers $v_{k,l} \in \mathbb{R}^{|S_{kl}|}$ are applied as constraints of each area in (6). The set Γ_k denotes the areas sharing the variables $x_k[l]$ with area k, the penalty parameter $\rho > 0$ is an empirically chosen constant in linear PSSE. The penalty parameter will not determine the results, but it will affect the convergence rate in the linear PSSE model. Considering t as the iteration index, ADMM can be performed through the following calculations:

$$x_k^{t+1} := arg \ \min \ Ł(x_k, x_{kl}^t; v_{k,l}^t \mid x_k \in \chi_k) \tag{7a}$$

$$x_{kl}^{t+1} := arg \ \min \ Ł \ (x_k^{t+1}, x_{kl}; v_{k,l}^t) \tag{7b}$$

$$v_{k,l}^{t+1} = v_{k,l}^t + \rho(x_k^{t+1}[l] - x_{kl}^{t+1}), \forall\, k, \ell. \tag{7c}$$

In the first ADMM step illustrated in (7a), each area updates their own states in iteration $t+1$ by minimizing their local objective function. This is done using information from auxiliary variables x_{kl} and Lagrange multipliers $v_{k,l}$ from the previous iteration t as shown in (7b) and (7c). To further simplify ADMM iterations, an updated expression of (7) was presented in [38] in the following format:

$$x_k^{t+1} = (H_k^T H_k + \rho D_k)^{-1} (H_k^T z_k + \rho D_k p_k^t) \tag{8a}$$

$$s_k^{t+1}(i) := \frac{1}{|\Gamma_k|} \sum_{\ell \in \Gamma_k} x_l^{t+1}(i), \forall\, i \ with \ \Gamma_k \neq \emptyset \tag{8b}$$

$$p_k^{t+1}(i) = p_k^t(i) - \frac{x_k^t(i) + s_k^t(i)}{2}, \forall\, i \ with \ \Gamma_k \neq \emptyset. \tag{8c}$$

In (8a), each area k has a diagonal matrix D_k with (i_{th}, i_{th}) entry $|\Gamma_k|$. $|\Gamma_k|$ is zero when the corresponding states are not shared by other neighbor area. Variable p_k is a transformed multiplier vector which gather information from Lagrange multiplier $v_{k,l}$, which has the same size of x_k. In (8b), s_k gathers the exchanged state values from neighboring shared buses. Meanwhile, p_k^{t+1} collects current s_k^t and then will be used to fix local state x_k in the next iteration as shown in (8c), $x_k(i)$ denotes each entry of $x_k[l]$. p_k is recursively calculated by eliminating Lagrange multiplier $v_{k,l}$, hence, the final expression for p_k is presented in the following equation:

$$p_k^{t+1}(i) = 1/|\Gamma_k^i| \sum_{l \in \Gamma_k^i} (x_{kl}^t(i) - v_{k,l}^t(i)/\rho) \tag{9}$$

Through this presented distributed linear power system state estimation framework, the objective function minimization in (8a) and update of transformed Lagrange multipliers p_k are performed in local control centers. Exchanged state information gathering is completed through a coordinator between neighboring areas. In this framework, only the information of boundary shared states is required to be exchanged. From (8a), one can see no information of measurements or regression matrix is needed to perform ADMM circulations.

3. Data integration for actual load characteristics from Electricity Reliability Council of Texas (ERCOT)

Up to 2021, the Electric Reliability Council of Texas (ERCOT) manages the flow of electric power to more than 26 million Texas customers representing about 90 percent of the state's electric load. As the independent system operator for the region, ERCOT schedules power on an electric grid that connects more than 46,500 miles of transmission lines and 710 generation units.

In power industries, optimal dispatch is based on load prediction models that use historic data. Once load profile for day ahead is confirmed, generation units are scheduled accordingly. On the other hand, a load profile is a chart to illustrate variation in demand during a specific time. Generation companies use this information to plan how much power they will need to generate for an optimal dispatch at any given time. In this paper, the load information for IEEE 118-bus system is updated on the basis of a load modeling technique which is based on the ERCOT customer load profile curves. In order to obtain a realistic time series of the true state variables (bus voltages and angles), the measurements data (including real power flow, reactive power flow, power injection and voltage) are generated using power system physical structure which coordinates the load information from industrial daily profile. Actual daily load information used is shown in Fig. 1. In Fig. 1, one can see customer peak demand is at noon time and decreases in the afternoon. After 17:00, the demand increases again and finally goes to a lower level at night time.

In addition, the load zone map of ERCOT is shown in Fig. 2. Area 1 denotes western connection; Area 2 denotes northern connection and Rayburn Electric Cooperative; Area 3 includes southern connection, Houston area, CPS Energy, Austin Energy and Lower Colorado River Authority.

4. Nonlinear distributed PSSE model

The nonlinear state estimator is based on the nonlinear measurement model as described in (1). However, the linear D-PSSE illustrated in above section is not suitable to solve the nonlinear problem, since one will need to consider gradient function iteratively instead of directly calculating the new state vector x_k^t by recorded measurements z_k as shown in (8a). In this section, a new nonlinear distributed PSSE model is presented.

The same problem expression is used as shown in (2). However, $h_k(x_k)$ is a nonlinear model which is used to perform estimation of the corresponding nonlinear measurements z_k. To solve the nonlinear problem, an extra step to calculate the correction of state vector is presented based on Eqs. (5) and (7). Considering the simplified ADMM-based distributed state estimation from (8a), one can expand (7a) and rewrite this equation as follows:

$$\min_{x_k} f_k(x_k) + \rho/2 \sum_{\Gamma_k^i \neq \emptyset} |\Gamma_k^i|(x_k(i) - p_k^t(i))^2 \tag{10}$$

for all k and i = 1, 2, …, Γ_k, with $\Gamma_k^i \neq \emptyset$.

In [21], the first order optimal condition for model (3) can be written as:

$$g_k(x_k) = \partial J(x_k)/\partial x_k = -\sum_{j=1}^{m}\left(\frac{z_{kj} - h_{kj}(x_k)}{\sigma_{kj}}\right)\frac{\partial h_{kj}(x_k)}{\partial x_k} = 0, \tag{11}$$

where σ_{kj} is the (k, j)th element of the measurement error covariance matrix R_k, $g_k(x)$ denotes the gradient of $J_k(x_k)$. The solution of above nonlinear equation $g_k(x_k) = 0$ can be found by performing the Newton–Raphson method. Meantime, the gradient function can be approximated by using Taylor expansion:

$$g_k(x_k + \triangle x_k) \simeq g_k(x_k) + G_k(x_k) \triangle x_k, \tag{12}$$

where $G_k(x_k)$ is the Hessian matrix of $J_k(x_k)$ of area k. Collecting first Taylor derivative, $G_k(x_k)$ becomes:

$$G_k(x_k) = H_k^T(x_k)R_k^{-1}H_k(x_k), \tag{13}$$

where H_k is the Jacobian matrix of objective function.

Using above equations, one can derive the first optimal condition for nonlinear state estimator from (10):

$$g_k(x_k) = H_k^T(x_k)R_k^{-1}H_k(x_k)x_k^t - H_k^T R_k^{-1} z + \rho D_k x_k^t - \rho D_k p_k^t = 0. \tag{14}$$

Rearrange Eq. (14):

$$(H_k^T(x_k)R_k^{-1}H_k(x_k) + \rho D_k)x_k^t = H_k^T R_k^{-1} z + \rho D_k p_k^t. \tag{15}$$

The nonlinear state estimate x_k^{t+1} of area k is then obtained by the following iterative process:

$$(H_k^T(x_k)R_k^{-1}H_k(x_k) + \rho D_k) \triangle x_k^t = H_k^T R_k^{-1} r_k^t + \rho D_k \triangle p_k^t, \tag{16a}$$

$$\triangle p_k^t = p_k^t - p_k^{t-1}, \tag{16b}$$

$$x_k^{t+1} = x_k^t + \triangle x_k^t. \tag{16c}$$

$r_k^t = z - h(x)$ denotes the measurement residue in the tth iteration which is used as incremental value $\triangle z_k$ of measurement z_k. One will notice $\triangle p_k^t$ is not a nonlinear model based vector as r_k^t which is shown in (9), so the state estimate updating will have a direct derivation of the gradient through the above model. The next section will solve this problem through adapting the penalty parameter ρ by analyzing the Lagrange multiplier residue and primal residue of ADMM. In this section, a conclusive model of nonlinear PSSE is presented as the following:

$$\triangle x_k^t = (H_k^T H_k + \rho D_k)^{-1}[H_k^T r_k + \rho D_k(p_k^t - p_k^{t-1})] \tag{17a}$$

$$x_k^{t+1} = x_k^t + \triangle x_k^t \tag{17b}$$

$$s_k^{t+1}(i) := \frac{1}{|\Gamma_k|}\sum_{\ell \in \Gamma_k} x_l^{t+1}(i), \forall i \ with \ \Gamma_k \neq \emptyset \tag{17c}$$

$$p_k^{t+1}(i) = p_k^t(i) - \frac{x_k^t(i) + s_k^t(i)}{2}, \forall i \ with \ \Gamma_k \neq \emptyset. \tag{17d}$$

5. Adaptive penalty parameter

In ADMM based linear D-PSSE, the penalty parameter ρ is an empirically defined constant. This parameter will not affect the final estimation results, however it will affect the convergence performance. In nonlinear PSSE, however, this penalty parameter will decide the convergence process and final results since ρ is used to determine the step length in the approximated gradient function which is derived from the Taylor expansion (17). As mentioned in the previous section, the incremental value of the transformed Lagrange multiplier $\triangle p_k^t$, which is not a nonlinear based vector since it is only the difference of p_k^t in two following iterations, will cause insufficient state estimate updating due to lacking an appropriate penalty parameter as a fixing property. One can notice the penalty parameter ρ is a multiplier of $\triangle x_k^t$ as shown in (17), so setting up a unique and constant penalty parameter for each area is not practical for the nonlinear PSSE. In order to accurately update shared state variables and improve the convergence, a method based on adaptive penalty parameter is presented to update ρ in every iteration.

The necessary and sufficient optimal conditions for the ADMM problem (4) are primal and dual feasibility [47]. In presented model (17), primal feasibility is defined as

$$\rho(x_k^*[l] - x_{kl}^*) = 0, \tag{18}$$

where $x_k^*[l]$ is the sub-state of x_k which consists of the overlapping states with area l, x_{kl} is auxiliary variable between the pair of overlapping areas k and l. One can define the difference between vector $x_k[l]$ and x_{kl} as the primal residue at iteration t shown in following:

$$r_k^{prim^t} = \rho(x_k^t[l] - x_{kl}^t), \ for \ all \ k, l. \tag{19}$$

The value of the primal residue r_k^{prim} illustrates how far the current shared states in area k are from the auxiliary vector x_{kl} determined by area k itself and neighboring areas l together during each iteration. Generally, one can also understand the primal residue as the difference between previous Lagrange multiplier $v_{k,l}^t$ and the multiplier $v_{k,l}^{t+1}$ at the current iteration (7c).

Dual feasibility is defined as:

$$0 \in \partial f(x^*) + v_{k,l}^*. \tag{20}$$

Here, ∂ denotes the subdifferential vector [47]. When function f is differentiable, then subdifferential ∂f can be replaced by $\bigtriangledown f$ and $\in$ can be replaced by $=$.

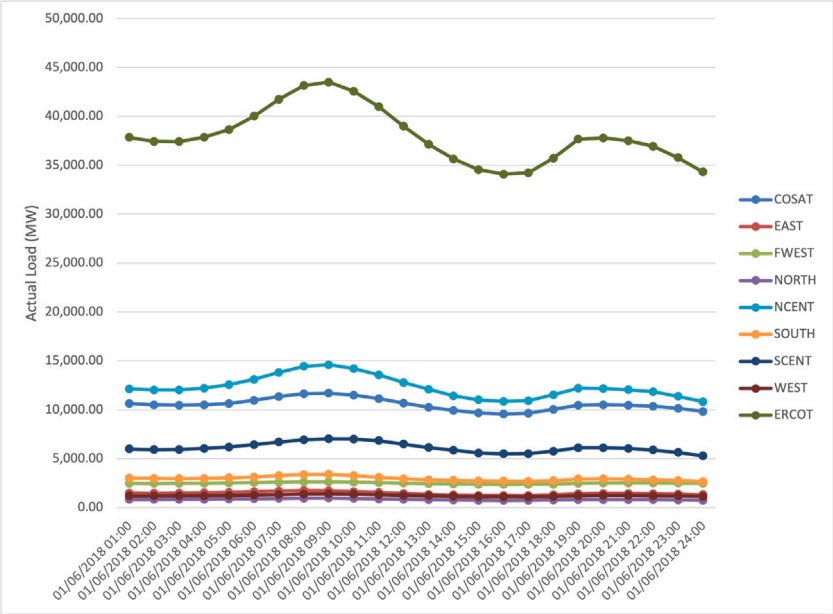

Fig. 1. Actual daily load profile from ERCOT.

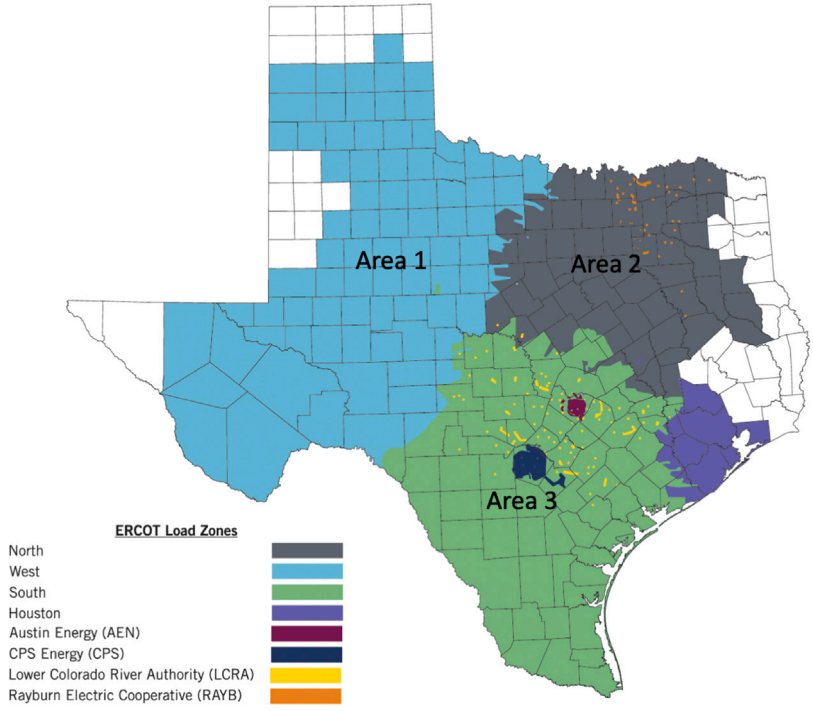

Fig. 2. Electricity Reliability Council of Texas (ERCOT) load zone map.

Since x^{t+1} minimizes Ł$(x_k, x_{kl}^t; v_{k,l}^t)$ as shown in (7) by definition, let us expand Eq. (7a):

$$0 \in \partial f(x^{t+1}) + v_{k,l}^t + \rho(x_k^{t+1}[l] - x_{kl}^t) \tag{21}$$

We can eliminate vector $x_k^{t+1}[l]$ by adding the primal residue (19) at $t+1$ iteration as an extra term. This leads to:

$$0 = \partial f(x^{t+1}) + v_{k,l}^t + r_k^{prim(t+1)} + \rho(x_{kl}^{t+1} - x_{kl}^t) \tag{22}$$

Further, to eliminate the Lagrange multiplier $v_{k,l}^t$ in the tth iteration and primal residue $r_k^{prim(t+1)}$ in $t+1^{th}$ iteration, one can replace these two terms using (7c). Then

$$0 = \partial f(x^{t+1}) + v_{k,l}^{t+1} + \rho(x_{kl}^{t+1} - x_{kl}^t), \tag{23}$$

or equivalently,

$$\partial f(x^{t+1}) + v_{k,l}^{t+1} = \rho(x_{kl}^t - x_{kl}^{t+1}). \tag{24}$$

One should notice that the left hand side of the above equation is exactly the condition of dual feasibility optimization as shown in (20). While the right hand side can be expressed as follows:

$$r_k^{dual} = \rho(x_{kl}^t - x_{kl}^{t+1}), \tag{25}$$

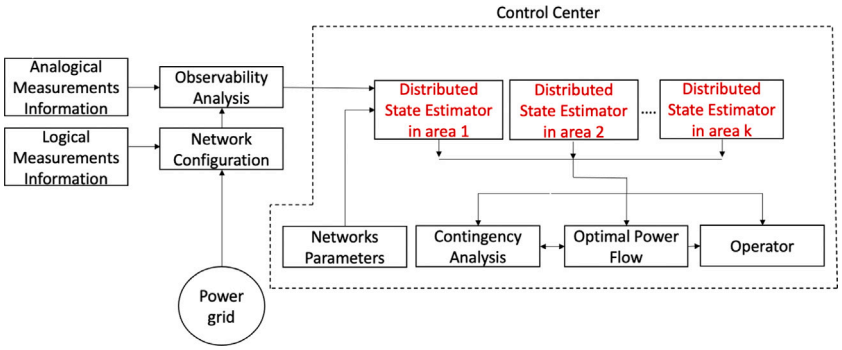

Fig. 3. Flowchart of distributed SE process adapted from [22].

and r_k^{dual} can be viewed as the dual residue in the dual feasibility condition (20). From the above expression, one can see the dual residue is actually the difference between the auxiliary variable x_{kl}^t at tth iteration and x_{kl}^{t+1} at $t+1^{th}$ iteration which is used as reference state between two neighbor areas.

To improve the gradient deviation in the presented nonlinear state estimation update in (17), the adaptive penalty parameter ρ is used to balance the primal residue r_k^{prim} and the dual residue r_k^{dual}. For balance of these two residues, the novelty here is to adjust the penalty parameter ρ_k in each area to constrain $\left\|r_k^{prim}\right\| \approx \left\|r_k^{dual}\right\|$, which means different areas will have penalty parameters themselves to monitor the iterative updating process. From [27], an increase in ρ strengthens the penalty term, leading to smaller primal residues and larger dual residues; a decrease in ρ will yield larger primal residue but smaller dual residue.

To constrain these two residues, $\left\|r_k^{prim}\right\| \approx \left\|r_k^{dual}\right\|$, which means they will simultaneously converge to 0. An adaptive penalty parameter method is completed by the following algorithm considering r_k^{prim} and r_k^{dual}.

$$\rho_k^{t+1} = \begin{cases} \upsilon^{inc}\rho_k^t & \left\|r_k^{prim}\right\|_2 > \mu \left\|r_k^{dual}\right\|_2 \\ \rho_k^t / \upsilon^{dec} & \left\|r_k^{dual}\right\|_2 > \mu \left\|r_k^{prim}\right\|_2 \\ \rho_k^t & otherwise \end{cases} \tag{26}$$

This equation shows each area has their own penalty parameter ρ_k. They could start with the same penalty parameter or they could not since ρ_k will adjust itself in each area. When the system converges, ρ_k will converge to a fixed status based on r_k^{prim} and r_k^{dual}. The algorithm has three parameters with the following constraints: $\mu > 1$, $\upsilon^{inc} > 1$, and $\upsilon^{dec} > 1$. These are typically chosen to be μ=10, υ^{inc}=2, υ^{dec}=2. The idea of penalty parameter updating is meant to maintain the norm of the primal residue and dual residue to a relative low value for each other so they can both converge to 0. Process of presented distributed method is shown in Fig. 3.

6. Case study

In this case study, presented algorithm is applied on two different distributed system scenarios. Validation is done using the IEEE 14-bus and 118-bus systems with the load information from ERCOT. The measurement data set used for IEEE 14-bus system consists 84 measurements obtained from MATPOWER [49], leading to a global redundancy level GRL = 3.11, leading to local GRLs for area 1, 2, 3 and 4 are 1.72, 1.76, 1.76 and 1.30. For the IEEE 118-bus test system the measurement data set consists of 573 measurements, leading to the global GRL = 2.44, local GRLs for area 1, 2, 3 are 2.19, 2.14 and 2.36. By using the daily load information shown in Fig. 1 from ERCOT, measurement data set contains a variation on the basis of ERCOT customer demand. In the process of generating measurement data by integrating load information, load condition is updated every four seconds. Hence, there are 21 600 samples for every daily load profile. For detection, Chi-square test which is widely used in power industries is implemented to evaluate the system performance. System parameters are found in [50].

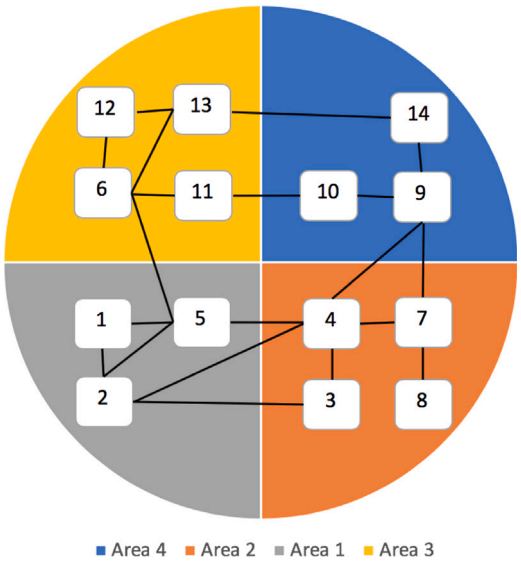

Fig. 4. IEEE 14 bus system separated into 4 areas and recorded measurements configuration adapted from [37].

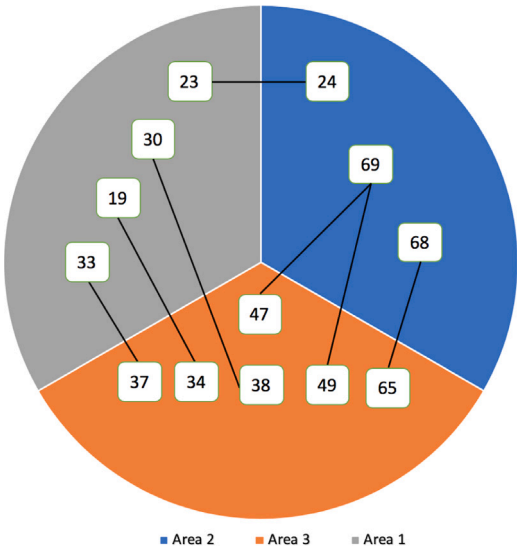

Fig. 5. Distributed topology of IEEE 118-bus system adapted from [48].

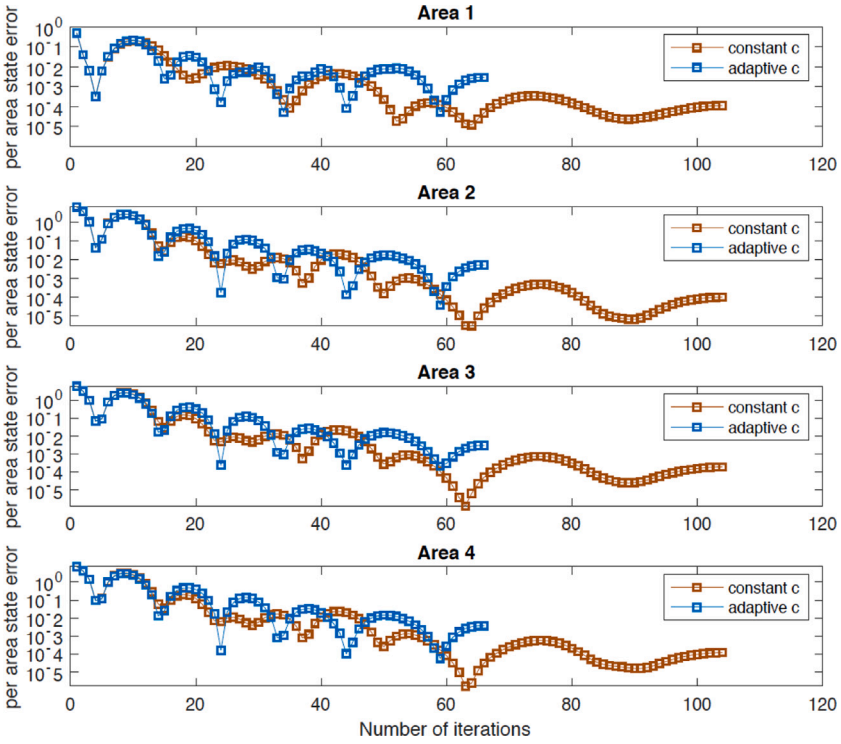

Fig. 6. State error curve in each iteration for IEEE 14 bus system with starting penalty parameter 100 000.

6.1. Distributed PSSE scenario I

In this case, we use the distributed topology shown in Fig. 4 for the IEEE 14-bus system. Measurement noise is simulated as independent zero-mean Gaussian distribution with standard deviation equal to 1% of each measurement. To better illustrate the advantage of presented nonlinear PSSE model, different starting penalty parameter conditions will be considered. True states x_{lf} from load flow [49] are used as benchmark. Per state error curve rate is calculated by $e_k^t = log_{10}^{\left\|x_k - x_{lf}\right\|_2}$.

In Fig. 6, a scenario where starting penalty parameter $\rho = 100\,000$ are used. Two different results are presented: In constant penalty parameter case, four areas shown in Fig. 4 have the same penalty parameter ρ and they will remain the same values until convergence using presented nonlinear PSSE model (17); in adaptive penalty parameter case, four areas have same starting values of ρ_k, however each area k update their ρ_k based on the presented adaptive model (26). From blue curve (constant penalty parameter), one can see system converge after 105 iterations when correction of states $\triangle x$ is smaller than 10^{-4}. After convergence, per area state error e_k^t for all four areas are below 10^{-3}. Meantime, in orange curve (adaptive penalty parameter), system converge at 64 iterations, while per area state error e_k^t is below 10^{-3} which is around the same as constant penalty parameter case, however using less iterations. Corrected value of penalty parameter in each area after convergence is presented in Table 1. One will see ρ_k in area 1 increase to 3 200 000, however decrease to 25000 and 3125 in area 3 and 4 instead, while remain the same starting value in area 2. This shows necessity to apply adaptive penalty parameter in nonlinear PSSE implementation, since different area has different sensitivity for shared information between interconnected areas. One should notice corrected penalty parameter shown in Table 1 does not mean these values are the optimal starting ρ_k for each area, since when system starts with a relatively small ρ_k, even ρ_k will adapt itself during convergence, later stage of PSSE process before convergence with larger ρ_k will fix the previews lost of small ρ_k to guarantee r_k^{prim} and r_k^{dual} are corrected in the same rate. So the optimal starting ρ_k is actually some value in the middle of starting value and corrected value after convergence. One should note that one will not need to find this optimal value in PSSE, like classical ADMM algorithm requires.

Table 1
Corrected penalty parameter after convergence with starting value of 100 000.

Corrected penalty parameter				
Penalty parameter	Area 1	Area 2	Area 3	Area 4
ρ_k	3 200 000	100 000	25 000	3125

To further demonstrate the advantage using the adaptive penalty parameter model (26) in nonlinear PSSE, the cumulative residue based objective function $J(x) = \sum_{k=1}^{K} J_k(x_k)$ performance in (4) with different starting ρ_k is presented in Fig. 7. In Fig. 7, orange scattered points shows penalty parameter ρ_k is changing from range of 80 000 to 300 000, when plotting objective value obtained after convergence, one will notice the performance of cumulated $J(x)$ are very stable where almost all values are near around 30. Whereas, constant penalty parameter based PSSE (blue scattered points) shows objective function value $J(x)$ will show a false positive of PSSE detection when ρ_k is getting larger. Using adaptive penalty parameter model in (26), objective function is free from correlating to ρ_k. From Fig. 7, one can also see the average centralized objective function solution 56.3067 is smaller than threshold value 75.6237. However, in presented distributed PSSE model, this value is decreased to 30, which characterizes a better performance.

6.2. Distributed PSSE scenario II

In this case study, system topology in Fig. 5 is used to test presented nonlinear PSSE model and adaptive penalty parameter algorithm. There are 3 interconnected areas in distributed IEEE 118-bus system as shown in this topology. The measurement data set for IEEE 118-bus system is generated with the changing load which contains information of daily customer demand from ERCOT, this measurement characteristics is shown in Fig. 8. Same noise as IEEE 14-bus system is used which is independent zero-mean Gaussian with standard deviation which is

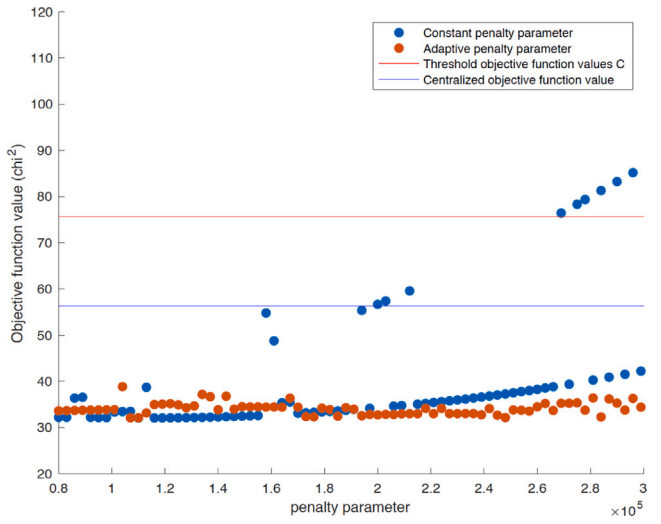

Fig. 7. Performance of objective function value with starting penalty parameter varying from 80 000–300 000.

1% of each measurement. Starting penalty parameter is set as 300 000. Fig. 9 show how per area state error behaves during each iteration for IEEE 118 bus system. Orange curve (using constant penalty parameter) shows system converges after around 47 iterations, per area state error for area 1,2,3 are around 10^0, 10^{-3}, 10^{-4}, while one can see the blue curve (using adaptive penalty parameter) converges with only 25 iterations, the same area state error at the same time. Blue curve shows the model in (26) has a fast convergence rate compared to constant penalty parameter based nonlinear PSSE. After convergence, ρ_k for area 1, 2 and 3 adapts to 600 000, 300 000 and 300 000 in Table 2. One can see ρ_k in area 1 increases, while remaining the same value as starting value for area 2 and 3. From Table 2, it is not clear to see how ρ_k adapts itself in nonlinear PSSE process, further analysis is done in the end of this section.

To evaluate the objective function behavior regarding the change of starting penalty parameter ρ_k, analysis is implemented with ρ_k starting values from 2500–800 000. In Fig. 10, the orange scattered points (adaptive penalty parameter based PSSE) illustrates a stable objective function distribution where all values are close to 300 which is not changing when enlarging ρ_k. On the other hand, blue scattered points appears in a little chaos, potentially causing false positives at the bad data analytic. For comparison with centralized PSSE solution, one can see all objective function values shown by orange points (adaptive penalty parameter) are below centralized solution which is 306.4442, which further highlights the advantage of presented distributed nonlinear PSSE model.

In [39], authors used state information x_k and consensus variables, which are calculated through the residue r_k and the Jacobian matrix from boundary areas, thus not a fully distributed solution. In the results shown in Table 3, one can see presented solution obtains an objective

Table 2
Corrected penalty parameter after convergence with starting value of 300 000.

Corrected penalty parameter			
Penalty parameter	Area 1	Area 2	Area 3
ρ_k	600 000	300 000	300 000

Table 3
Compared results.

	Objective function J(x)	Numbers of iteration
Presented algorithm (IEEE 14 bus system)	32.5765	63
Algorithm from [39] (IEEE 14 bus system)	43.5522	84
Presented algorithm (IEEE 118 bus system)	298.7467	25
Algorithm from [39] (IEEE 118 bus system)	300.7745	10

function value 32.5765, which is lower than the solution from [39], however using less iterations regarding to IEEE 14-bus system; For IEEE-118 system, presented solution obtains average J(x)=298.7467, which is also lower than 300.7745 from [39]. In this case, presented solution uses more iterations, however, process of neighboring areas exchanging information only requires states sharing, there is no information of neighboring Jacobian area and residue needed.

To present inner PSSE process of how penalty parameter ρ_k adapts to fix primal residue r_k^{prim} and dual residue r_k^{dual} for optimal solution, results from area 3 in IEEE 118-bus system is presented in Fig. 11. From (26), one can see if norm of primal residue is larger than μ times norm of dual residue, penalty parameter doubles, while norm of dual residue is larger than μ times norm of primal residue, ρ_k decrease by 2 times. In this model, μ is usually set as 10, so system can simply adapt ρ_k by determine if the value $\gamma = log_{\mu}^{\left\|r_k^{dual}\right\|/\left\|r_k^{prim}\right\|}$ is bigger than 1 or smaller than -1 or otherwise. If γ is larger than 1, then decrease ρ_k; If γ is smaller than -1, then increase ρ_k; Remain the same otherwise. From Fig. 12, ρ_k decrease at iteration 2, 8, 13 and 18 when γ is larger than 1 as shown in Fig. 11; while increase at iteration 26, 28, 29 and 32 when γ is smaller than -1.

Respectively, same test for a small starting penalty parameter is presented as follows. From Fig. 14, penalty parameter remain the same at the beginning when γ is within the limitation -1 to 1, however increases at iteration 10, 11, 13 and 14 when limitation is violated, as in Fig. 13.

After system convergence, the final bus voltage estimates of each area are accordingly shown in Figs. 15, 16, 17. The results shows the converged estimates are much close to power flow solution.

7. Conclusion

This paper presents a real-time industrial integration framework for a distributed nonlinear PSSE model based on alternating direction method of multiplier (ADMM). Adaptive penalty parameter model is further presented to eliminate correlation between system objective function value and starting value of penalty parameter chosen. Case

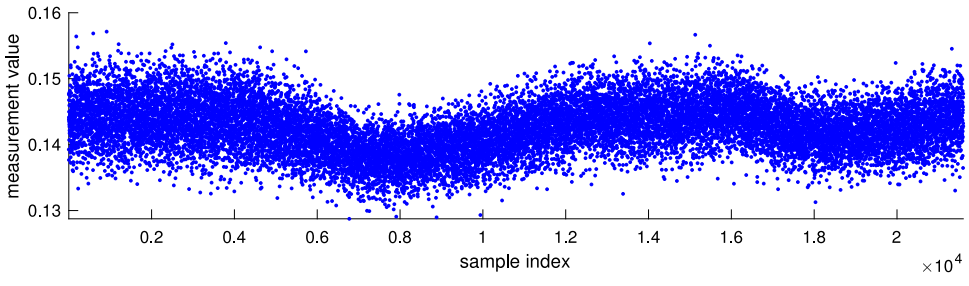

Fig. 8. An example of measurement characteristics by integrating load information.

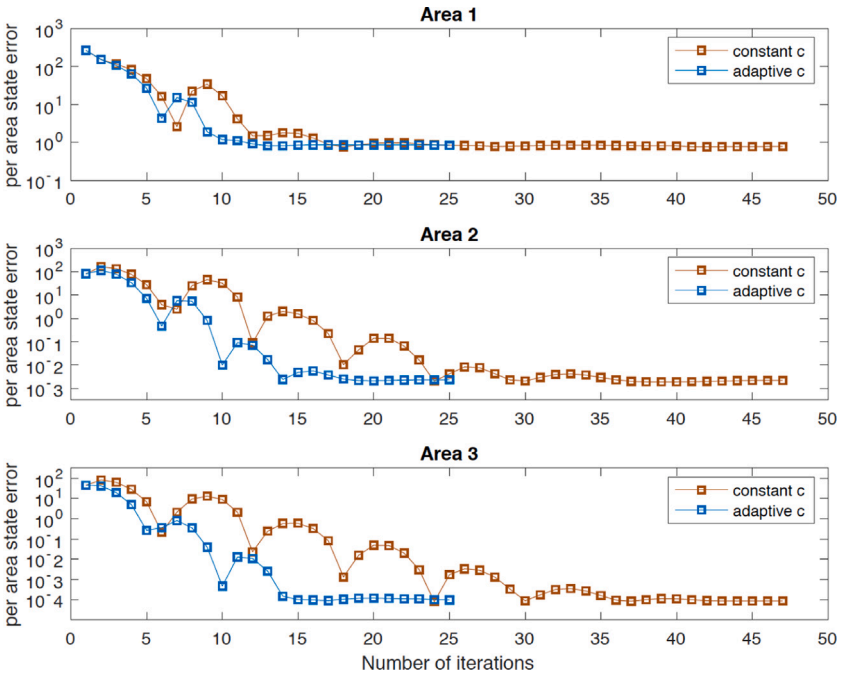

Fig. 9. State error curve in each iteration for IEEE 118 bus system.

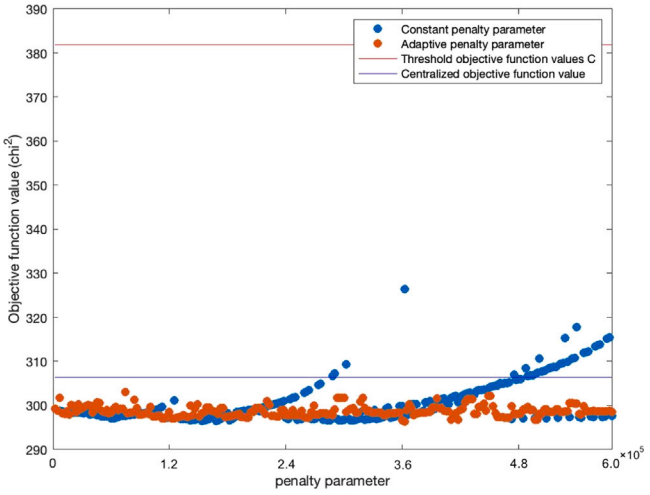

Fig. 10. Performance of objective function value with starting penalty parameter varying from 2500–600 000.

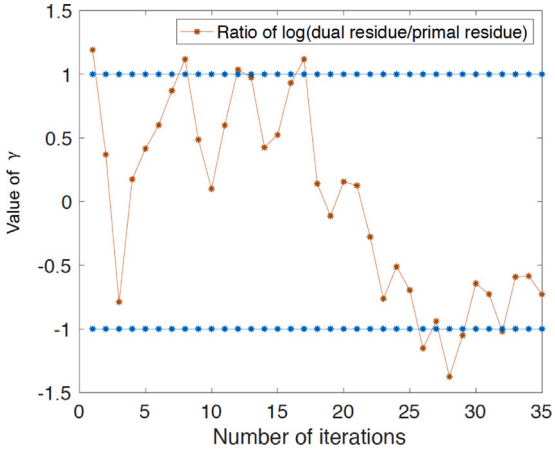

Fig. 11. Correlation of dual residue and primal residue with penalty parameter in iteration (starting with large ρ_k 800 000).

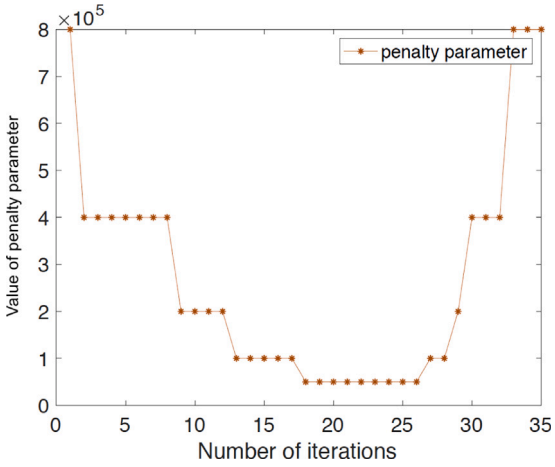

Fig. 12. Adapting performance of penalty parameter in iteration (starting with large ρ_k 800 000).

studies consider the IEEE 14-bus and IEEE 118-bus with the load information which is integrated from ERCOT daily load profile, highlighting presented model good performance of convergence rate and objective function behavior. The advantage of presented distributed PSSE model is final estimation solution performs better than centralized solution, and it allows any starting penalty parameter setting without any previews knowledge of power system. Still, the PSSE software using by power industries does not require major changes for the implementation of the distributed estimation model, only state values need to be exchanged between neighbor areas.

However, the modeling accuracy of power system physical topology in the proposed methodology is still limited considering the efficiency of information integration. With regard to our future work, the information of Phasor Measurement Unit (PMU) optimal allocation and Synthetic Measurement can be evaluated as additional features to test their impact on the performance of the model.

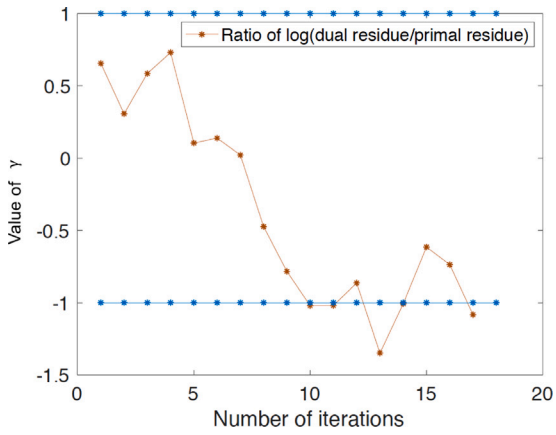

Fig. 13. Correlation of dual residue and primal residue with penalty parameter in iteration (starting with small ρ_k 20 000).

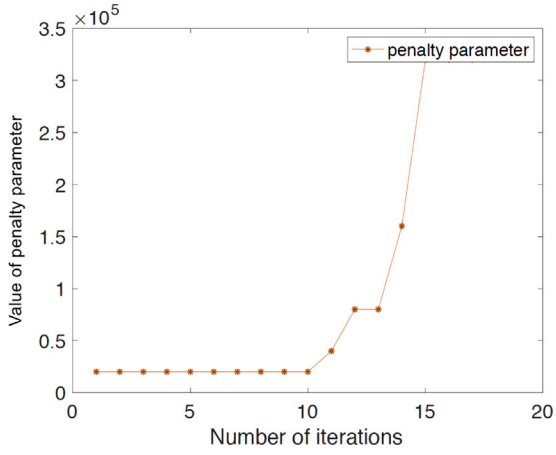

Fig. 14. Adapting performance of penalty parameter in iteration (starting with small ρ_k 20 000).

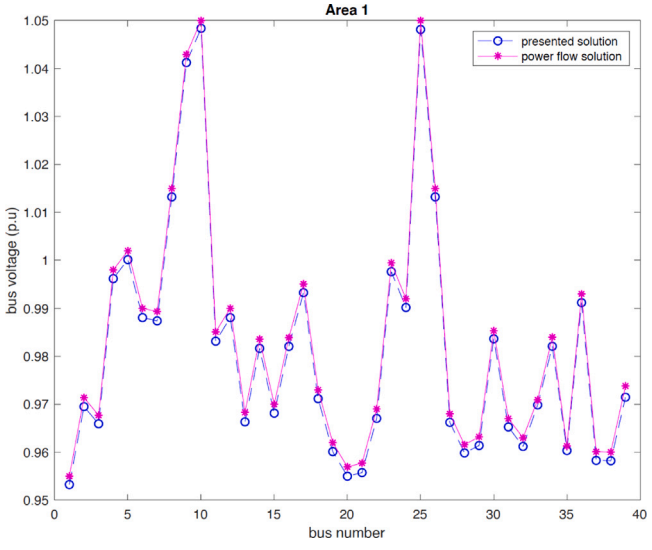

Fig. 15. Bus voltage in area 1.

Meanwhile, how to integrate the current algorithms with the nature-inspired algorithms so as to strengthen the overall effects, is a challenging and attractive issue.

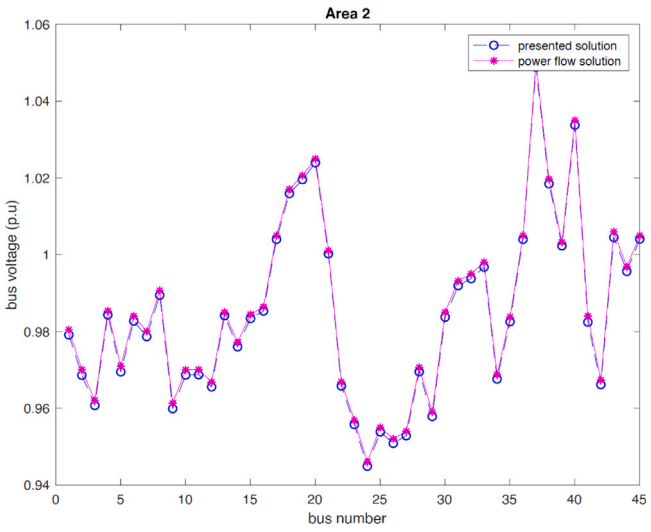

Fig. 16. Bus voltage in area 2.

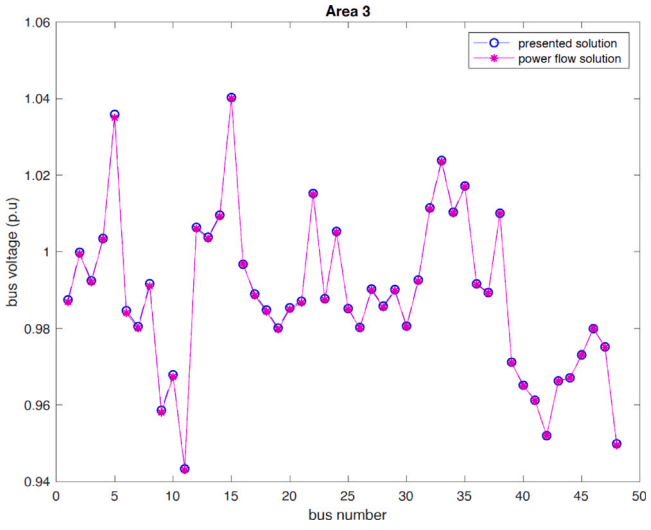

Fig. 17. Bus voltage in area 3.

CRediT authorship contribution statement

Tierui Zou: Conceptualization, Methodology, Software, Writing - original draft. **Nader Aljohani:** Software, Visualization, Investigation, Writing - review & editing. **Pan Wang:** Supervision, Visualization, Investigation, Writing - review & editing. **Arturo S. Bretas:** Supervision, Visualization, Investigation, Writing - review & editing. **Newton G. Bretas:** Supervision, Visualization, Investigation, Writing - review & editing.

Declaration of competing interest

The authors declare that they have no known competing financial interests or personal relationships that could have appeared to influence the work reported in this paper.

References

[1] L. Xu, Enterprise Integration and Information Architecture: A Systems Perspective on Industrial Information Integration, CRC Press, 2014.
[2] L. Xu, Inaugural issue editorial, J. Ind. Inf. Integr. 1 (2016) 1–2.

[3] L. Xu, Industrial information integration–an emerging subject in industrialization and informatization process, J. Ind. Inf. Integr. 17 (2020) 100128.

[4] Y. Chen, Industrial information integration—A literature review 2006–2015, J. Ind. Inf. Integr. 2 (2016) 30–64.

[5] Y. Chen, A survey on industrial information integration 2016–2019, J. Ind. Inf. Integr. 5 (01) (2020) 33–163.

[6] T. Chen, Z. Cai, X. Zhao, C. Chen, X. Liang, T. Zou, P. Wang, Pavement crack detection and recognition using the architecture of segnet, J. Ind. Inf. Integr. 18 (2020) 100144.

[7] A.A. Nazarenko, J. Sarraipa, L.M. Camarinha-Matos, C. Grunewald, M. Dorchain, R. Jardim-Goncalves, Analysis of relevant standards for industrial systems to support zero defects manufacturing process, J. Ind. Inf. Integr. 23 (2021) 100214.

[8] U. Subudhi, S. Dash, Detection and classification of power quality disturbances using gwo elm, J. Ind. Inf. Integr. 22 (2021) 100204.

[9] A. Bretas, N. Bretas, S. Braunstein, A. Rossoni, R. Trevizan, Multiple gross errors detection, identification and correction in three-phase distribution systems WLS state estimation: A per-phase measurement error approach, Electr. Power Syst. Res. 151 (2017) 174–185.

[10] D. Duan, L. Yang, L.L. Scharf, Phasor state estimation from PMU measurements with bad data, in: 2011 4th IEEE International Workshop on Computational Advances in Multi-Sensor Adaptive Processing (CAMSAP), IEEE, 2011, pp. 121–124.

[11] W. Xu, M. Wang, J. Cai, A. Tang, Sparse recovery from nonlinear measurements with applications in bad data detection for power networks, 2011, arXiv preprint arXiv:1112.6234.

[12] A.S. Bretas, N.G. Bretas, B. Carvalho, E. Baeyens, P.P. Khargonekar, Smart grids cyber-physical security as a malicious data attack: An innovation approach, Electr. Power Syst. Res. 149 (2017) 210–219.

[13] Y. Liu, P. Ning, M.K. Reiter, False data injection attacks against state estimation in electric power grids, ACM Trans. Inf. Syst. Secur. 14 (1) (2011) 13.

[14] O. Kosut, L. Jia, R.J. Thomas, L. Tong, Malicious data attacks on the smart grid, IEEE Trans. Smart Grid 2 (4) (2011) 645–658.

[15] S.A. Zonouz, K.M. Rogers, R. Berthier, R. Bobba, W.H. Sanders, T.J. Overbye, SCPSE: Security-oriented cyber-physical state estimation for power grid critical infrastructures., IEEE Trans. Smart Grid 3 (4) (2012) 1790–1799.

[16] Y. Mo, T.H.-J. Kim, K. Brancik, D. Dickinson, H. Lee, A. Perrig, B. Sinopoli, Cyber–physical security of a smart grid infrastructure, Proc. IEEE 100 (1) (2011) 195–209.

[17] P. Wang, L. Xu, S.-M. Zhou, Z. Fan, Y. Li, S. Feng, A novel Bayesian learning method for information aggregation in modular neural networks, Expert Syst. Appl. 37 (2) (2010) 1071–1074.

[18] P. Wang, J. Wang, J. Zhang, Methodological research for modular neural networks based on "an expert with other capabilities", J. Glob. Inf. Manag. (JGIM) 26 (2) (2018) 104–126.

[19] D. Luenberger, An introduction to observers, IEEE Trans. Automat. Control 16 (6) (1971) 596–602, http://dx.doi.org/10.1109/TAC.1971.1099826.

[20] R.E. Kalman, A new approach to linear filtering and prediction problems, Trans. ASME-J. Basic Eng. 82(Series D) (1960) 35–45.

[21] A. Monticelli, State Estimation in Electric Power Systems: A Generalized Approach, Springer Science & Business Media, 2012.

[22] T. Zou, A.S. Bretas, C. Ruben, S.C. Dhulipala, N. Bretas, Smart grids cyber-physical security: Parameter correction model against unbalanced false data injection attacks, Electr. Power Syst. Res. 187 (2020) 106490.

[23] T. Zou, A.S. Bretas, N. Aljohani, N.G. Bretas, Malicious data injection attacks: A relaxed physics model based strategy for real-time monitoring, in: 2019 North American Power Symposium (NAPS), IEEE, 2019, pp. 1–6.

[24] N.G. Bretas, A.S. Bretas, A two steps procedure in state estimation gross error detection, identification, and correction, Int. J. Electr. Power Energy Syst. 73 (2015) 484–490.

[25] A. Gómez-Expósito, A. de la Villa Jaén, C. Gómez-Quiles, P. Rousseaux, T. Van Cutsem, A taxonomy of multi-area state estimation methods, Electr. Power Syst. Res. 81 (4) (2011) 1060–1069.

[26] L. Zhao, A. Abur, Multi area state estimation using synchronized phasor measurements, IEEE Trans. Power Syst. 20 (2) (2005) 611–617.

[27] S. Boyd, N. Parikh, E. Chu, Distributed Optimization and Statistical Learning Via the Alternating Direction Method of Multipliers, Now Publishers Inc, 2011.

[28] R. Ebrahimian, R. Baldick, State estimation distributed processing [for power systems], IEEE Trans. Power Syst. 15 (4) (2000) 1240–1246.

[29] A. Gomez-Exposito, A. Abur, A. de la Villa Jaen, C. Gomez-Quiles, A multilevel state estimation paradigm for smart grids, Proc. IEEE 99 (6) (2011) 952–976.

[30] A.J. Conejo, S. de la Torre, M. Canas, An optimization approach to multiarea state estimation, IEEE Trans. Power Syst. 22 (1) (2007) 213–221.

[31] S. Naka, T. Genji, T. Yura, Y. Fukuyama, A hybrid particle swarm optimization for distribution state estimation, IEEE Trans. Power Syst. 18 (1) (2003) 60–68.

[32] M. Rana, L. Li, S. Su, Distributed state estimation using RSC coded smart grid communications, IEEE Access 3 (2015) 1340–1349.

[33] C. Liu, Y. Wang, D. Zhou, X. Shen, Minimum-variance unbiased unknown input and state estimation for multi-agent systems by distributed cooperative filters, IEEE Access 6 (2018) 18128–18141.

[34] H. Zhang, B. Zhang, A. Bose, H. Sun, A distributed multi-control-center dynamic power flow algorithm based on asynchronous iteration scheme, IEEE Trans. Power Syst. 33 (2) (2018) 1716–1724.

[35] S. Iwamoto, M. Kusano, V. Quintana, Hierarchical state estimation using a fast rectangular-coordinate method (power system analysis computing), IEEE Trans. Power Syst. 4 (3) (1989) 870–880.

[36] D.E. Marelli, M. Fu, Distributed weighted least-squares estimation with fast convergence for large-scale systems, Automatica 51 (2015) 27–39.

[37] G.N. Korres, A distributed multiarea state estimation, IEEE Trans. Power Syst. 26 (1) (2010) 73–84.

[38] V. Kekatos, G.B. Giannakis, Distributed robust power system state estimation, IEEE Trans. Power Syst. 28 (2) (2013) 1617–1626.

[39] S. Xia, Q. Zhang, J. Jing, Z. Ding, J. Yu, B. Chen, H. Wu, Distributed state estimation of multi-region power system based on consensus theory, Energies 12 (5) (2019) 900.

[40] L. Xie, D.-H. Choi, S. Kar, H.V. Poor, Fully distributed state estimation for wide-area monitoring systems, IEEE Trans. Smart Grid 3 (3) (2012) 1154–1169.

[41] J. Du, S. Ma, Y. Wu, H.V. Poor, Distributed hybrid power state estimation under PMU sampling phase errors, IEEE Trans. Signal Process. 62 (16) (2014) 4052–4063.

[42] R. Carli, M. Dotoli, Using the distributed proximal alternating direction method of multipliers for smart grid monitoring, in: 2017 13th IEEE Conference on Automation Science and Engineering (CASE), 2017, pp. 418–423.

[43] N. Bretas, A.S. Bretas, The extension of the Gauss approach for the solution of an overdetermined set of algebraic non linear equations, IEEE Trans. Circuits Syst. II: Express Briefs 65 (9) (2018) 1269–1273.

[44] N. Bretas, A. Bretas, A.C. Martins, Convergence property of the measurement gross error correction in power system state estimation, using geometrical background, IEEE Trans. Power Syst. 28 (4) (2013) 3729–3736.

[45] N. Bretas, A. Bretas, S. Piereti, Innovation concept for measurement gross error detection and identification in power system state estimation, IET Gener. Transm. Distrib. 5 (6) (2011) 603–608.

[46] N.G. Bretas, S.A. Piereti, A.S. Bretas, A.C. Martins, A geometrical view for multiple gross errors detection, identification, and correction in power system state estimation, IEEE Trans. Power Syst. 28 (3) (2013) 2128–2135.

[47] A. Kusraev, S. Kutateladze, Local convex analysis, J. Sov. Math. 26 (4) (1984) 2048–2087.

[48] B. Wang, X. Fang, X. Zhao, H. Chen, Bi-level optimization for available transfer capability evaluation in deregulated electricity market, Energies 8 (12) (2015) 13344–13360.

[49] R.D. Zimmerman, C.E. Murillo-Sánchez, D. Gan, MATPOWER: A MATLAB Power System Simulation Package, Vol. 1, Manual, Power Systems Engineering Research Center, Ithaca NY, 1997.

[50] R. Christie, Power Systems Test Case Archive, Electrical Engineering dept., University of Washington, 2000.